



Sustinere

Journal of Environment and Sustainability

Volume 8 Number 2 (2024) 142-151

Print ISSN: 2549-1245 Online ISSN: 2549-1253

Website: <https://sustinerejes.com> E-mail: [sustinere.jes@uinsaid.ac.id](mailto:sustinere.jes@uinsaid.ac.id)

## RESEARCH PAPER

# Slot-die coating method in organic solar panel and evaluation in polluted air

Tohid Irani\*, Hedieh Deyhim

*Dept. of Civil Engineering, School of Civil & Environmental Engineering, University of Shiraz PNU, Shiraz, Iran*

Article history:

Received 25 February 2024 | Accepted 14 August 2024 | Available online 31 August 2024

**Abstract.** Renewable energy sources and pollution have a direct effect on each other. Solar panels development could enhance the adoption of green energy sources and contribute to a cleaner environment. Today's third generation organic photovoltaic panels (OPVs) offer good efficiency, low fabrication costs, and can be produced rapidly using slot-die coating methods. These advantages make OPVs increasingly attractive for broadening solar energy consumption. Therefore, related studies are being conducted to achieve this goal. This study aimed to evaluate real-world performance of OPVs in polluted air by testing a fully slot-die-coating OPV module in Tehran's polluted environment, specifically at four air quality control stations. The results showed a power conversion efficiency (PCE) of 6.3% under standard test condition (STC) and maximum power output of 0.189 W in 5×6 cm module, which include ITO/PET, PEI, P3HT-PCBM, PEDOT-PSS, and AGNW layers. Testing in polluted environment revealed a significant decrease in current and maximum power (P<sub>max</sub>) due to reduced sunlight reaching the module's surface. P<sub>max</sub> dropped to 0.0229 W at least polluted site in Masodieh Street and to 0.0173 W at the most polluted site in Shahr-e Rey Street.

**Keywords:** Slot dies coating; Air pollution; Organic solar panels; Sun irradiation power.

## 1. Introduction

The development of green energy sources is increasingly valuable for energy production, particularly in addressing the pollution problems associated with fossil fuels and enhancing sustainability development (Heeger, 2010; Liang et al., 2010). By generating electricity through solar panels, air pollution can be reduced, contributing to a healthier environment. Unlike other energy sources, such as gas power plants and fossil fuels, solar power plants do not require water to produce electricity (Syam, 2023). Continue reliance on non-renewable energy sources like fossil fuels may eventually lead to natural disasters. Utilizing solar energy reduces dependence on non-renewable resources and helps maintain a healthy and intact planet.

The increase in pollutants and carbon compounds from non-renewable sources in the atmosphere has led to various adverse effects on human health (Falkowska, 2016). Solar energy can help reduce carbon emissions and ultimately mitigate the effects of global warming. However, the output power of a solar panels may decrease due to pollution on the module's surface, with this decrease quantified by a reduction factor related to air pollution. The extent of power

\*Corresponding author. E-mail: [tohidirani68@gmail.com](mailto:tohidirani68@gmail.com)

DOI: <https://doi.org/10.22515/sustinere.jes.v8i2.389>

reduction due to pollution varies by climate and is particularly significant in highly polluted areas, such as large cities. For example, pollution can reduce solar panel efficiency by approximately 3-5% ([Serenelli et al., 2023](#)). The concentration of airborne particulates reduces the light that solar panels can capture, and these particulates have the greatest effect on reducing the output power by contaminating the surface of solar panels.

The production of solar electricity in developing countries is presents a major challenge, because air pollution is an uncontrollable environmental issue in this region, and the cost of regularly cleaning solar panels is often not economically feasible.

The process of generating electricity in a solar power plant is completely ecological and does not produce pollutants that harm the environment. Among renewable and non-renewable sources, solar energy is considered one of the most efficient. Solar power plants are generally categorized into two main types: solar thermal power plants and solar photovoltaic (PV) power plants. These power plants consist of interconnected solar cells that absorb sunlight and generate direct electric current (DC) electricity due to advancements in solar cell technology. Solar panels are connected in parallel, forming strings that are linked to a current inverter ([Mahamat & Margoum, 2020](#)). The inverter converts the DC from the solar cells into alternating current (AC). This energy is then directed to a transformer, where the voltage and current intensity is adjusted, allowing energy to be transmitted to consumption centers through power grid lines.

Air pollution, especially in urban areas, can significantly affect the efficiency of solar panels. Therefore, the impact of pollution on solar panels should be considered during their design. An increase in air pollution concentration can significantly reduce the performance characteristics of photovoltaic panels. For example, the efficiency of monocrystalline silicon panels decreased by 37.74, 55.87 and 66.61% under different levels of pollution compared to clean air conditions ([Rao & Dubey, 1990](#)). The corresponding values for polycrystal panels were 25.70, 51.49 and 58.05%, respectively ([Jenkal et al., 2023](#)). In this research, the efficiency of organic photovoltaic (OPV) panels in polluted sites in Tehran was recorded.

Using green energy sources like solar PV panels offer greater flexibility in energy production while contributing to a cleaner environment. However, pollution can negatively impact the energy production of OPVs panels ([Kim et al., 2007](#)). As third generation solar panels, OPVs are emerging as a promising green energy technology, offering advantages over conventional solar panels, such as silicon panel and CIGS panels, which are made from inorganic materials ([Y. Li et al., 2018](#)). OPVs use polymer materials that are more accessible, and their fabrication processes are less expensive and easies to operate compared to traditional methods like sputtering and co-evaporation ([Brabec, 2004](#)).

Lower efficiency of OPVs compared to inorganic solar panels is more significant challenge, even beyond the panel's longevity in environmental conditions ([Hong et al., 2013](#)). The disadvantages of OPVs are affected by the materials and methods used in the fabrication ([Hoth et al., 2007](#)). The absorption, conductivity, and durability of the materials are crucial for achieving higher efficiency and longer operational lifespans, Additionally, the specifics of the fabrication methods can significantly escalate process quality ([Krebs et al., 2009](#)). In this study a slot-die coating method was employed using an indium tin oxide/polyethylene terephthalate (ITO/PET) substrate, with Polyetherimide (PEI) as Electron Transport Layer (ETL) and Poly(3,4-ethylenedioxythiophene) polystyrene sulfonate: Polystyrene sulfonate (PEDOT:PSS) as Hole Transport Layer (HTL). The PV2000:PCBM blend serves as photoactive layer, and Anisotropic Grayscale Nanowire (AGNW) was used as the top electrode, all fabricated using the slot-die method to achieve a flexible OPV with a 20 cm<sup>2</sup> active area. This method is recognized as a simple and cost-effective approach, utilizing readily accessible materials commonly used in other tests of OPVs.

The efficiency of OPVs is significantly affected by solar irradiation and temperature ([Carlé & Krebs, 2013](#)). Most research is conducted under standard test condition (STC), which include a

solar irradiation of 1000 w/m<sup>2</sup>, a temperature of 25°C, and a standard pressure of 1.5 AM in a controlled laboratory environment. However, these conditions often differ significantly from real-world environment, and active area used in tests is typically much smaller than in actual operation ([Jayakrishnan & Shouri, 2014](#)). Lower irradiation levels decrease output power and particularly affects short-circuit current (I<sub>sc</sub>), while open-circuit voltage (V<sub>oc</sub>) remains close to STC results ([Garluna, 2022](#)). Another important factor is temperature; at higher temperature (above 25°C), the V<sub>oc</sub> decreases, although the open-circuit current (I<sub>oc</sub>) remains close to STC values.

A reviewing of researches on OPVs technology clearly shows that enhancing efficiency is a primary goal ([Moonen et al., 2012](#)). Researchers have explored various material combinations and methods to achieve significant advancements in this field ([Mazzio & Luscombe, 2015](#)). In one study, a slot-die coating method was used to fabricate OPVs, resulting in a Power Conversion Efficiency (PCE) of 7.5%, with the top electrode applied via vacuum evaporation ([Chang et al., 2019](#)). In another study, [Liu et al. \(2022\)](#) tested a slot-die coating method for preparing AGNW transparent films on PET substrates, yielding promising results for large-scale applications as top electrodes in OPVs. Several studies have concluded that using full slot-die coating and roll-to-roll processes for large scale OPV fabrication can produce good PCEs ([Tsuchiya et al., 2010](#)), although the achieved efficiencies remain relative low.

The impact of solar irradiance on PCE is an essential factor in assessing OPV performance, particularly under cloudy and rainy conditions, as reduce irradiance clearly lead to lower efficiency ([Hallum et al., 2023](#)). In this study, a full slot-die coating process was used to fabricate all layers of OPVs using the same printable method, aiming to produce flexible OPVs with lower production costs. Additionally, real-ambient tests were conducted in the polluted air of Tehran to analysis the effect of irradiance on PCE. The scale of this study was limited to an active area of 30 cm<sup>2</sup>, with dead area neglected.

## 2. Material and method

### 2.1. Experimental

The basic substrate, made of ITO/PET, was fabricated using the radio frequency (RF) sputtering method, with a thickness of 0.176 mm and 75% transparency, and flexibility. This substrate was used to coat ETL, photoactive layer, HTL, and top electrode. The substrate's flexibility, conductivity, and good transmittance, as studied by researchers ([Leong et al., 2020](#)), made it ideal for this application. The transmittance curve, shown in Figure 1, indicates about 80% transmittance.

Before coating, the substrate was pre-cleaned using acetone, Isopropyl Alcohol (IPA), detergent, and deionized water in ultra-sonication process. The cleaned substrate was then ready for the ETL layer, which was made using Polyethylenimine (PEI) polymer. The PEI was coated with at a speed of 2 m/min in a preheated substrate at 120 C° for 10 min, achieving a 40 nm thick ETL layer.

Next, the photoactive layer was formed on the ETL using a blend of Poly(3-hexylthiophene) - [6,6]-Phenyl-C<sub>61</sub>-butyric acid methyl ester (P3HT-PCBM) ([Hu & Gesquiere, 2009](#)). P3HT and PCBM mixed in 1 mg/ml dichlorobenzene at a ratio of 1:0.8 to create slot-die coating ink, with all materials purchased from Merck. The slot-die coating process for the Photoactive layer was performed at a speed of 1-1/5 m/min with coating gap of 0.15 mm on the preheated ETL layer at 60 C°, resulting in a 150-200 nm thick P3HT-PCBM layer.

The HTL was made of Poly(3,4-dimethylphenylthiophene) (PCDOT)-PSS, also purchased from Merck. The solution was prepared by dissolving PCDOT-PSS in Isopropanol (IPA) at a ratio of 1:2. The final ink was coated on the preheated proactive layer at 70 C° with a speed of 0.5 m/min and coating gap of 0.15 mm for 3 min, then dried at 120 C° to reach a thickness of 150-200 nm.

The top electrode layer, composed of AGNW, could be processed via vacuum evaporation. However, in this study, the slot-die coating method was used to achieve an 40 nm thick top connector layer ([X. Li et al., 2023](#)). To form the final layer, 10 mg/ml AGNW was dissolved in 8 mg

hydroxypropyl-methyl-cellulose, 1 mg/ml Zonyl Fso-100, and 10 ml deionized water, mixed for 1 hour to create the ink solution of top electrode. Coating was performed on the preheated HTL layer at 45 C°, with a speed 5 mm/s and a solution charge rate of 1 ml/min, then allowed to air-dry. The slot-die coating machine was equipped to deposit five cells, each 1 cm wide and 6 cm long, with adequate measurement facilities to monitor thickness, speed, and drying conditions consistently. Pneumatic pumps were used to supply the ink solution into the injection space. [Figure 2](#) shows the organic module structure used in this study.

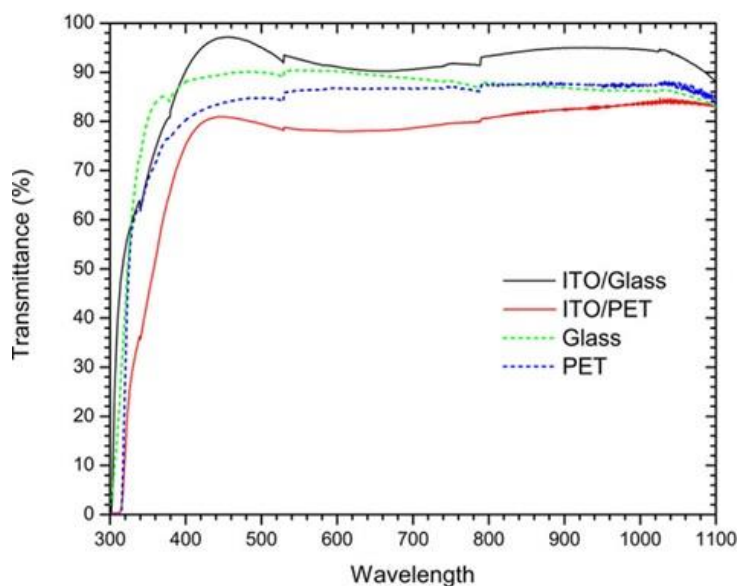


**Figure 1.** Transmittance of ITO on glass and PET substrate ([Leong et al., 2020](#))

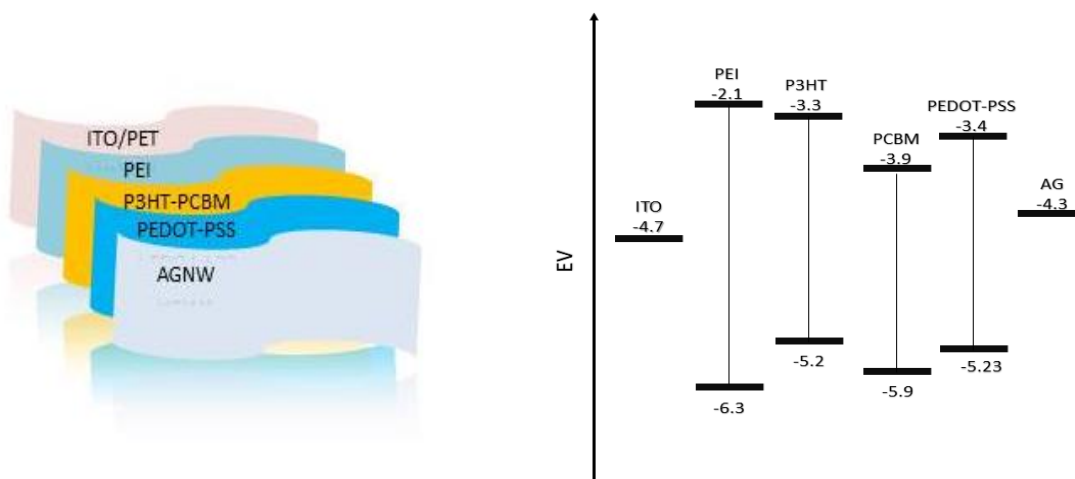


**Figure 2.** The OPV's Energy Band and Structure

## 2.2. Methodology

The operation of a fabricated OPV module was evaluated at four air quality monitoring station in Tehran city, Iran. The sites were selected based on pollution levels, population density, wind speed, and topography, resulting in the choice of locations in the north, east, center, and south of Tehran to test OPV parameters and power output ([Yousefi et al., 2019](#)). The air quality index (AQI) pollutants measured included Particulate Matter 2.5 (PM<sub>2.5</sub>), Particulate Matter 10

(PM<sub>10</sub>), Sulfur Dioxide (SO<sub>2</sub>), Nitrogen Dioxide (NO<sub>2</sub>), Carbon Monoxide (CO), and Ozone (O<sub>3</sub>). These measurements were taken under identical conditions to record the OPVs maximum current (Im), maximum voltage (Vm), short-circuit current (Isc), and open-circuit voltage (Voc). The parameters were obtained using a Prova-1011 solar panel meter. Solar irradiance was recorded at temperatures between 7°C and 13°C at each test station using a DT-1307 solar power meter (measured in w/m<sup>2</sup>). The tests were conducted on January 2, 2024 in Tehran. [Table 1](#) shows the Environmental Protection Agency (EPA) Air Quality Index (AQI) standards used in this study.

**Table 1.** Air pollution Index based on EPA ([www.EPA.gov/enviroatias](http://www.EPA.gov/enviroatias))

Air Quality Index Levels of Health Concern	Numerical Value	Meaning
Good	0 to 50	Air quality is considered satisfactory and air pollution poses little or no risk
Moderate	51 to 100	Air quality acceptable; however, for some pollutants there may be a moderate health concern for a very small number of people who are unusually sensitive to air pollution
Unhealthy for sensitive groups	101 to 150	Members of sensitive groups may experience health effects. The general public is not likely to be affected
Unhealthy	150 to 200	Everyone may begin to experience health effects, members of sensitive groups may experience more serious health effects
Very unhealthy	201-300	Health warnings of emergency conditions. The entire population is more likely to be affected
Hazardous	301 to 500	Health alert: everyone may experience more serious health

The module parameters were analyzed under STC with an irradiance of 1000 W/m<sup>2</sup>, an air mass (AM) of 1.5, and temperature of 25°C, using a solar simulator chamber ([Garluna, 2022](#)). The performance results in polluted environment were evaluated based on current (I), voltage (V), current density (J), fill factor (FF), power conversion efficiency (PCE), and power parameters. Additionally, UV-Vis-NIR spectroscopy (Shimadzu, UV-3600 Plus) was employed to determine the absorption of Bulk Heterojunction (BHJ) layer using the Incident Photon-to-Current Efficiency (IPCE) measurement method. MATLAB was also used for plotting and analyzing the data.

### 3. Result and discussion

#### 3.1. Slot die coating result

This experiment utilized a common BHJ layer OPV to demonstrate the effect of solar irradiance, particularly in polluted air conditions. The OPV was fabricated on an IOT/ PET substrate with over 75% transparency and flexibility. The device comprised with four layers: an ETL made of PEI, a BHJ layer made of P3HT-PCBM, a HTL made of PEDOT-PSS, and a top connector made of silver nanowires (AGNW). The layers were deposited using a die coating technique, where the coating ink solution was prepared and applied accordingly.

The OPV module was analyzed under STC and showed a promising PCE of 6.3% over an active area of 30 cm<sup>2</sup>. The module's dead area was disregarded to achieve a five-cell module with dimensions of 5×6 cm<sup>2</sup>. The STC results demonstrated the following parameters: FF of 65%, Isc of 71 mA, Voc of 4.1 V, Im of 48 mA, Vm of 3.9 V, (Short-Circuit Current Density) Jsc of 2.36 mA/cm<sup>2</sup>, and maximum power (P<sub>max</sub>) of 0.182 W, as shown in [Table 2](#).

During the coating process, the BHJ layer required greater precision due to the low viscosity of the solution, leading to slower coating and drying speeds to achieve the desired PCE ([Ganesan et al., 2019](#)). To analyze the BHJ layer made of P3HT-PCBM, UV-vis spectroscopy ([Najafi et al., 2021](#)) was conducted at a substrate temperature of 60°C, showing regular absorption curves that indicate crystallization and drying effects from the die coating process at a speed of 1- 1/5 mm/min. Although the results are not directly comparable to inorganic modules like CIGS flexible

panels (Mufti et al., 2020), the fast fabrication process, low material costs, and efficient methods make this OPV more favorable than CIGS modules. Figure 3 shows fabricated OPV in Flexible form with a 30 cm<sup>2</sup> active area (including the dead area) comprising five cells of 1×6 cm on a 10 cm<sup>2</sup> ITO/PET substrate.

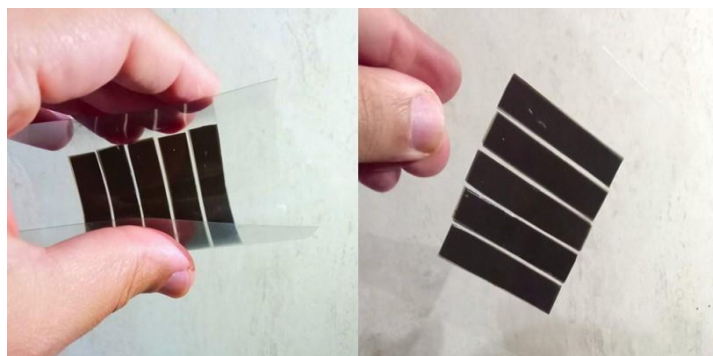


Figure 3. Fabricated OPV in Flexible form and 30 cm<sup>2</sup>

Table 2. Standard condition results

Pin (w/m <sup>2</sup> )	Voc (v)	Isc (mA)	Jsc (mA/cm <sup>2</sup> )	Vm (v)	Im (mA)	P <sub>max</sub> (w)	PCE%	FF%
1000	4.1	71	2.36	3.6	52	0.189	6.3	65

### 3.2. Air quality control station data analysis

Four air quality control stations in Tehran were selected based on topography, wind speed, and pollution levels to ensure a diverse set of data on air pollution and its impact on solar irradiance. The station chosen were Ponak station (north), Sharif station (center), Masodieh station (east), and Shahr-e Rey station (south). The temperature during test period, conducted between 11.00 am and 1:00 pm, ranged from 7°C to 13°C, which was lower than the standard 25°C.

High polluted levels were observed for PM<sub>2.5</sub> and PM<sub>10</sub> compared to other pollutions. The results were classified according to EPA's color-coded AQI to represent air quality conditions and visibility ranges, both of which directly affect solar irradiance consequently lower the efficiency of the OPV module.

Figure 4, based on data from Table 3, illustrates the recorded pollution levels and corresponding solar irradiance (Pin) at each station. The figure clearly shows an inverse relationship between AQI and Pin, indicating that higher pollution levels lead to lower output power, which negatively impacts the OPV efficiency.

Table 3. Four air quality control station data

St/Data	PM <sub>2.5</sub> (µg/m <sup>3</sup> )	PM <sub>10</sub> (µg/m <sup>3</sup> )	SO <sub>2</sub> (µg/m <sup>3</sup> )	NO <sub>2</sub> (µg/m <sup>3</sup> )	O <sub>3</sub> (µg/m <sup>3</sup> )	CO (µg/m <sup>3</sup> )	Pin (w/m <sup>2</sup> )
Masodieh st	85	99	10	69	8	10	129
Ponak st	126	86	17	87	13	16	117
Sharif st	157	100	18	73	8	21	110
Shahr-e Rey st	171	112	18	53	14	13	103

### 3.3. Discussion

Using the DT-1307 solar power meter, solar irradiance was recorded at station, and simultaneously, the panel parameters were obtained with the Prova-1011. The data shows a clear inverse relationship between increasing pollution levels and decreasing solar power, as expected. The highest power was recorded at Masodieh station, where 129 w/m<sup>2</sup> was measured,

corresponding to about 13% of the power received under STC. This occurred under a yellow AQI status, with PM<sub>10</sub> levels at 90 µg/m<sup>3</sup>.

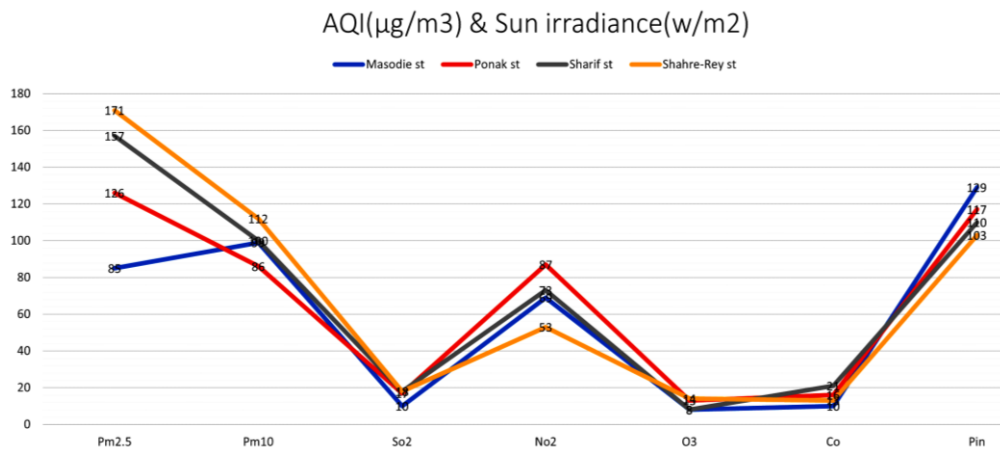


**Figure 4.** Pollution index recorded in stations and irradiance Pin

A noticeable decline in  $I_{sc}$ ,  $I_m$ ,  $V_{oc}$ , and  $V_m$  was observed due to the reduction in incoming solar power. Although a slight decrease in PCE was also noted, the FF remained constant, indicating linear changes in current and voltage. A reduction in solar power to 117 w/m<sup>2</sup> at Ponak station (with an AQI of PM<sub>2.5</sub> at 126 µg/m<sup>3</sup>) and 110 w/m<sup>2</sup> at Sharif station (with an AQI of PM<sub>2.5</sub> at 157 µg/m<sup>3</sup>) led to further decreases in current and voltage, all of which exhibited gradual, linear changes.

The most significant decrease was recorded at Shahr-e Rey station, where the AQI for PM<sub>2.5</sub> reached 171 µg/m<sup>3</sup>, and solar power dropped to 103 w/m<sup>2</sup>, which is close to 10% of the STC power in laboratory conditions. The results clearly indicate that PM is the most effective pollutant in reducing the voltage and current (V-I), with the changes being linear when temperature is below 25°C. The data shows a slight change in voltage but a significant change in current, aligning with expected outcomes.

While the PCE changes slightly and may be negligible in large-scale applications,  $P_{max}$  exhibits substantial changes, showing a direct relationship between  $P_{max}$  and the solar power input (Pin). Another important factor is the visibility range, based on the EPA index, and its impact on solar power quality, which warrants further investigation.

The complete results are presented in Table 4. Figure 5a-b show the Current-Voltage curves for each station and their respective air quality, vividly illustrating the direct relationship between irradiance and input power, and the maximum power output compared to the STC curve. Additionally, Figure 5c-d-e display the Current Density-Voltage curves under STC and real irradiance conditions, and the IPCE-Absorbance curve as a function of wavelength, which was obtained through spectroscopy for the BHJ layer.

**Table 4.** Module operation data in air pollution

Pin (w/m <sup>2</sup> )	VoC (v)	Isc (mA)	Jsc (mA/cm <sup>2</sup> )	Vm (v)	Im (mA)	P <sub>max</sub> (w)	PCE%	FF%
129	3.60	9.70	0.32	3.55	6.45	0.0229	5.91	64.9
117	3.58	8.80	0.29	3.55	5.80	0.0206	5.86	65.0
110	3.58	8.07	0.27	3.54	5.30	0.0188	5.69	64.8
103	3.55	7.40	0.24	3.50	4.82	0.0173	5.60	64.8

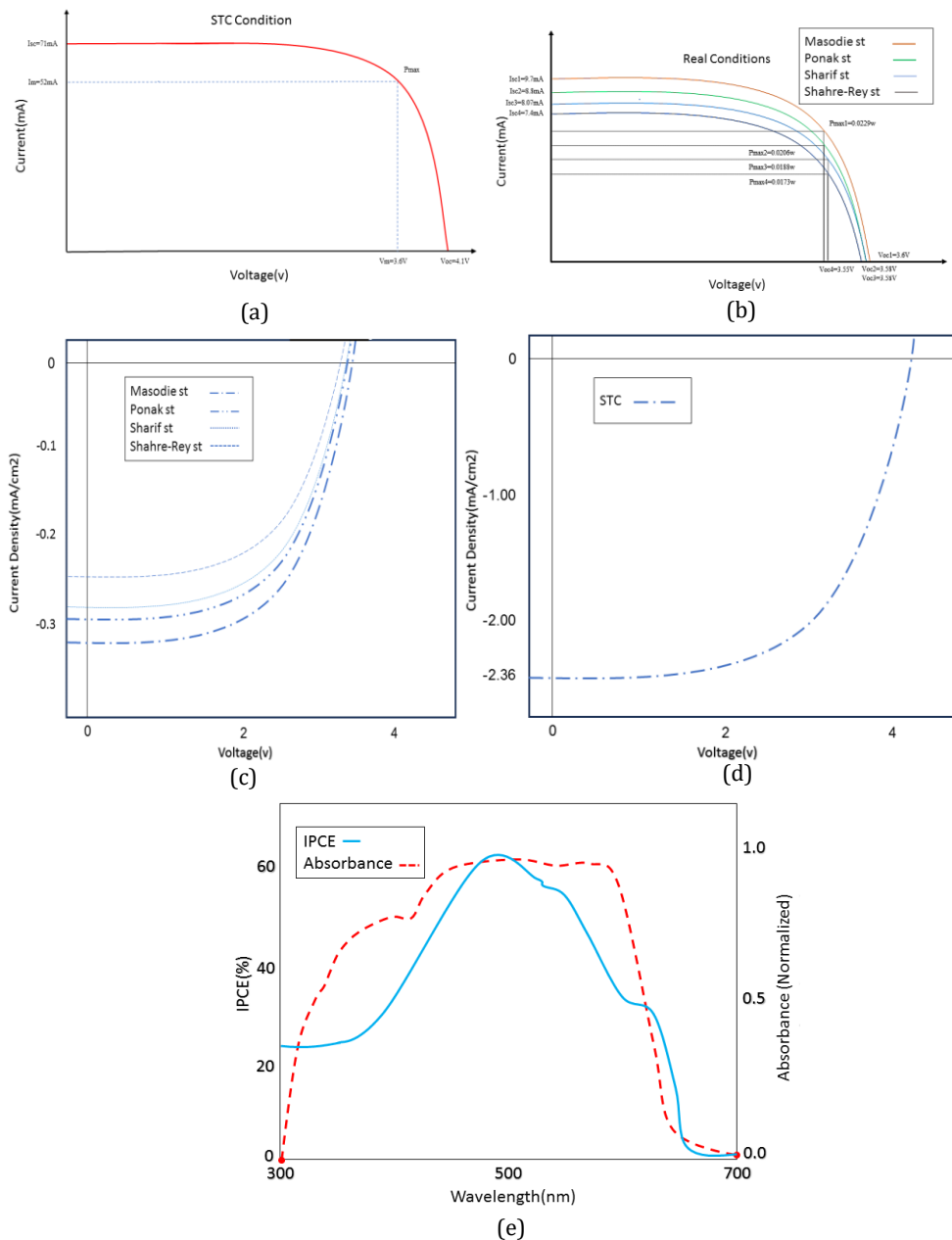


**Figure 5.** Current Voltage curve in a-STC and b-Real Condition in air pollution, Current Density Voltage Cure in c-STC and d-Real condition of air pollution, e-IPCE-Absorbance-Wavelength curve of P3DT-PCBM

The figures clearly illustrate the experimental results, demonstrating regular and expected changes consistent with similar research and established theories. Based on absorbance theories related to electron operation effects on the conductivity and efficiency of deposition materials, the OPVs performance indicates increased absorbance and efficiency across various wavelengths. This suggests that the OPV is approaching a high-quality standard, as evidence by the successful outcomes of experiment.

#### 4. Conclusion

Organic solar panels, as part of third generation photovoltaic technologies, require further research and experimentation to enhance their efficiency and stability. However, they are increasingly becoming a common energy source due to their lower costs and ease of fabrication



using methods like slot die coating method for producing relatively efficient OPVs and tested them in a real air polluted environment to evaluate the impact of pollution on performance parameters and efficiency. Four air quality control sites in Tehran were selected, and pollution data were analyzed alongside recorded OPV operation data. The results indicated a direct effect of air pollution, particularly PMs pollution, on OPV parameters such as current and maximum power (P<sub>max</sub>), primarily due to the reduction in solar irradiance. To mitigate this issue, STC for PCEs should be improved, as this would provide a more accurate assessment under polluted conditions, even at lower irradiance levels (below 1,000 w/m<sup>2</sup>) while maintaining a temperature at or below 25°C.

### Acknowledgment

The authors are very grateful all the members of the research and thanks the following reviewers to review this article.

### References

- Brabec, C. J. (2004). Organic photovoltaics: technology and market. *Solar Energy Materials and Solar Cells*, 83(2), 273–292. <https://doi.org/10.1016/j.solmat.2004.02.030>
- Carlé, J. E., & Krebs, F. C. (2013). Technological status of organic photovoltaics (OPV). *Solar Energy Materials and Solar Cells*, 119, 309–310. <https://doi.org/10.1016/j.solmat.2013.08.044>
- Chang, Y.-M., Liao, C.-Y., Lee, C.-C., Lin, S.-Y., Teng, N.-W., & Huei-Shuan Tan, P. (2019). All solution and ambient processable organic photovoltaic modules fabricated by slot-die coating and achieved a certified 7.56% power conversion efficiency. *Solar Energy Materials and Solar Cells*, 202, 110064. <https://doi.org/10.1016/j.solmat.2019.110064>
- Falkowska, L. (2016). Environmental characteristics of gaseous pollutants and related adverse health effects. In *Synergic influence of gaseous, particulate, and biological pollutants on human health* (pp. 3–38). CRC Press.
- Ganesan, S., Mehta, S., & Gupta, D. (2019). Fully printed organic solar cells – a review of techniques, challenges and their solutions. *Opto-Electronics Review*, 27(3), 298–320. [http://czasopisma.pan.pl/Content/115265/PDF/opelre\\_2019\\_27\\_3\\_298-320.pdf](http://czasopisma.pan.pl/Content/115265/PDF/opelre_2019_27_3_298-320.pdf)
- Garluna, J. (2022). Measuring Solar Cell Efficiency: A Comparative Study of Energy Conversion Efficiency of Solar Cells of the Solar Electric Vehicle, STC-3 at the World Solar Challenge in Australia and at Test Drives on Sathorn Road in Bangkok, Thailand. *TENCON 2022 - 2022 IEEE Region 10 Conference (TENCON)*, 1–3. <https://doi.org/10.1109/TENCON55691.2022.9977549>
- Hallum, G. E., Kürschner, D., Eulenkamp, C., Auer, R., Hartmann, B., Schulz, W., & Huber, H. P. (2023). Indium tin oxide ultrafast laser lift-off ablation mechanisms and damage minimization. *Chang Optics Express*, 31(26), 43017–43034. <https://doi.org/10.1364/OE.504582>
- Heeger, A. J. (2010). Semiconducting polymers: the Third Generation. *Chem. Soc. Rev.*, 39(7), 2354–2371. <https://doi.org/10.1039/B914956M>
- Hong, S., Lee, J., Kang, H., & Lee, K. (2013). Slot-die coating parameters of the low-viscosity bulk-heterojunction materials used for polymer solar cells. *Solar Energy Materials and Solar Cells*, 112, 27–35. <https://doi.org/10.1016/j.solmat.2013.01.006>
- Hoth, C. N., Choulis, S. A., Schilinsky, P., & Brabec, C. J. (2007). High Photovoltaic Performance of Inkjet Printed Polymer:Fullerene Blends. *Advanced Materials*, 19(22), 3973–3978. <https://doi.org/10.1002/adma.200700911>
- Hu, Z., & Gesquiere, A. J. (2009). PCBM concentration dependent morphology of P3HT in composite P3HT/PCBM nanoparticles. *Chemical Physics Letters*, 476(1), 51–55. <https://doi.org/10.1016/j.cplett.2009.05.066>
- Jayakrishnan, R., & Shouri, P. V. (2014). Optimum Monochromatic Wavelengths for Solar Panel Testing and Conversion of Parameters to STC. *Bonfring International Journal of Power Systems and Integrated Circuits*, 4(2), 18–24. <https://doi.org/10.9756/BIJPSIC.4869>
- Jenkal, S., Oubella, M., Mouslim, S., Ajaâmour, M., & Alaoui, M. S. H. (2023). Extraction of Monocrystalline Silicon Photovoltaic Panel Parameters Based on Experimental Data. *NanoWorld Journal*, 9(S2), 460–465. <https://doi.org/10.17756/nwj.2023-s2-078>
- Kim, J. Y., Lee, K., Coates, N. E., Moses, D., Nguyen, T.-Q., Dante, M., & Heeger, A. J. (2007). Efficient Tandem Polymer Solar Cells Fabricated by All-Solution Processing. *Science*, 317(5835), 222–225.

- <https://doi.org/10.1126/science.1141711>
- Krebs, F. C., Gevorgyan, S. A., & Alstrup, J. (2009). A roll-to-roll process to flexible polymer solar cells: model studies, manufacture and operational stability studies. *Journal of Materials Chemistry*, 19(30), 5442–5451. <https://doi.org/10.1039/B823001C>
- Leong, C. Y., Yap, S. S., Ong, G. L., Ong, T. S., Yap, S. L., Chin, Y. T., Lee, S. F., Tou, T. Y., & Nee, C. H. (2020). Single pulse laser removal of indium tin oxide film on glass and polyethylene terephthalate by nanosecond and femtosecond laser. *Nanotechnology Reviews*, 9(1), 1539–1549. <https://doi.org/doi:10.1515/ntrev-2020-0115>
- Li, X., Yang, H., Du, X., Lin, H., Yang, G., Zheng, C., & Tao, S. (2023). High-Performance Layer-by-Layer organic solar cells enabled by Non-Halogenated solvent with 17.89% efficiency. *Chemical Engineering Journal*, 452, 139496. <https://doi.org/10.1016/j.cej.2022.139496>
- Li, Y., Xu, G., Cui, C., & Li, Y. (2018). Flexible and Semitransparent Organic Solar Cells. *Advanced Energy Materials*, 8(7), 1701791. <https://doi.org/10.1002/aenm.201701791>
- Liang, Y., Xu, Z., Xia, J., Tsai, S.-T., Wu, Y., Li, G., Ray, C., & Yu, L. (2010). For the bright future-bulk heterojunction polymer solar cells with power conversion efficiency of 7.4%. *Advanced Materials (Deerfield Beach, Fla.)*, 22(20), E135-8. <https://doi.org/10.1002/adma.200903528>
- Liu, C., Zhang, X., Shan, J., Li, Z., Guo, X., Zhao, X., & Yang, H. (2022). Large-Scale Preparation of Silver Nanowire-Based Flexible Transparent Film Heaters by Slot-Die Coating. In *Materials* (Vol. 15, Issue 7, p. 2634). <https://doi.org/10.3390/ma15072634>
- Mahamat, C., & Margoum, E. hassane. (2020). A grid connected photovoltaic system using a parallel multilevel inverter: Optimal number of inverter cells. *Authorea*. <https://doi.org/10.22541/au.160504023.39489127/v1>
- Mazzio, K. A., & Luscombe, C. K. (2015). The future of organic photovoltaics. *Chemical Society Reviews*, 44(1), 78–90. <https://doi.org/10.1039/C4CS00227J>
- Moonen, P. F., Yakimets, I., & Huskens, J. (2012). Fabrication of Transistors on Flexible Substrates: from Mass-Printing to High-Resolution Alternative Lithography Strategies. *Advanced Materials*, 24(41), 5526–5541. <https://doi.org/10.1002/adma.201202949>
- Mufti, N., Amrillah, T., Taufiq, A., Sunaryono, Aripriharta, Diantoro, M., Zulhadjri, & Nur, H. (2020). Review of CIGS-based solar cells manufacturing by structural engineering. *Solar Energy*, 207, 1146–1157. <https://doi.org/10.1016/j.solener.2020.07.065>
- Najafi, L., Romano, V., Oropesa-Nuñez, R., Prato, M., Lauciello, S., D'Angelo, G., Bellani, S., & Bonaccorso, F. (2021). Hybrid Organic/Inorganic Photocathodes Based on WS<sub>2</sub> Flakes as Hole Transporting Layer Material. *Small Structures*, 2(3), 2000098. <https://doi.org/10.1002/sstr.202000098>
- Rao, M. V., & Dubey, P. S. (1990). Biochemical aspects (antioxidants) for development of tolerance in plants growing at different low levels of ambient air pollutants. *Environmental Pollution*, 64(1), 55–66. [https://doi.org/10.1016/0269-7491\(90\)90095-T](https://doi.org/10.1016/0269-7491(90)90095-T)
- Serenelli, L., Martini, L., Menchini, F., Izzì, M., & Tucci, M. (2023). Open circuit voltage reduction due to recombination at the heterojunction solar cell edge. *Solar Energy*, 258, 2–7. <https://doi.org/10.1016/j.solener.2023.04.027>
- Syam, D. J. (2023). Renewable and New Energy Sources for Electrical Power Generation: Solar Power Plants Wind Turbine Driven Power Plants Co-Generation Power Plants Biomass Based Power Plants Geo-Thermal Power Plants Tidal Energy Based Power Plants Fuel-Cells for Electrical . In *Electrical Power Generation*. CRC Press.
- Tsuchiya, T., Yamaguchi, F., Morimoto, I., Nakajima, T., & Kumagai, T. (2010). Microstructure control of low-resistivity tin-doped indium oxide films grown by photoreaction of nanoparticles using a KrF excimer laser at room temperature. *Applied Physics A*, 99(4), 745–749. <https://doi.org/10.1007/s00339-010-5633-0>
- Yousefi, S., Shahsavani, A., & Hadei, M. (2019). Applying EPA's instruction to calculate air quality index (AQI) in Tehran. *Journal of Air Pollution and Health*, 4(2), 81–86. <https://doi.org/10.18502/japh.v4i2.1232>